6462 *Biochemistry* **2010,** *49,* 6462–6472
DOI: 10.1021/bi100871b

BIOCHEMISTRY
including biophysical chemistry & molecular biology
Article

Isolation, Structure Elucidation, and Synergistic Antibacterial Activity of a Novel Two-Component Lantibiotic Lichenicidin from *Bacillus licheniformis* VK21[†,‡]

Zakhar O. Shenkarev, Ekaterina I. Finkina, Elina K. Nurmukhamedova, Sergey V. Balandin, Konstantin S. Mineev, Kirill D. Nadezhdin, Zoya A. Yakimenko, Andrey A. Tagaev, Yuri V. Temirov, Alexander S. Arseniev, and Tatiana V. Ovchinnikova*

Shemyakin and Ovchinnikov Institute of Bioorganic Chemistry, Russian Academy of Sciences, Miklukho-Maklaya str. 16/10, 117997 Moscow, Russia

Received May 30, 2010; Revised Manuscript Received June 25, 2010

ABSTRACT: A novel synergetic lantibiotic pair, Lchα (3249.51 Da) and Lchβ (3019.36 Da), termed lichenicidin VK21, was isolated from the producer strain *Bacillus licheniformis* VK21. Chemical and spatial structures of Lchα and Lchβ were determined. Each peptide contains 31 amino acid residues linked by 4 intramolecular thioether bridges and the N-terminal 2-oxobutyryl group. Spatial structures of Lchα and Lchβ were studied by NMR spectroscopy in methanol solution. The Lchα peptide displays structural homology with mersacidin-like lantibiotics and involves relatively well-structured N- and C-terminal domains connected by a flexible loop stabilized by a thioether bridge Ala11-S-Ala21. In contrast, the Lchβ peptide represents a prolonged hydrophobic α-helix flanked with more flexible N- and C-terminal domains. A lantibiotic cluster of the *Bacillus licheniformis* VK21 genome which comprises the structural genes, *lchA1* and *lchA2*, encoding the lantibiotics precursors, as well as the gene of a modifying enzyme *lchM1*, was amplified and sequenced. The mature peptides, Lchα and Lchβ, interact synergistically to possess antibiotic activity against Gram-positive bacteria within a nanomolar concentration range, though the individual peptides were shown to be active at micromolar concentrations. Our results afford molecular insight into the mechanism of lichenicidin VK21 action.

Massive-scale use of antibiotics resulted in the development of multiply resistant pathogens. During the recent years, the phenomenon of multiple pathogen resistance is recognized as a serious clinical problem driving scientists to search for new antibiotics for an effective management of relevant infections. Lantibiotics represent one of the promising classes of new antibacterial agents. These antimicrobial peptides are produced by Gram-positive bacteria and characterized by the presence of the thioether containing residues, termed lanthionine (Lan[1]) and 3-methyllanthionine (MeLan), as well as the unsaturated amino acids, such as 2,3-didehydroalanine (Dha) and 2,3-didehydrobutyrine (Dhb) (*1*). Lantibiotics are gene encoded, ribosomally synthesized, and post-translationally modified peptides. Interest in lantibiotics is prompted by their antimicrobial activity at nanomolar concentration levels. Development of resistance to lantibiotics is still unknown despite their widespread use as food preservation reagents for over 40 years (*1*).

A special group of lantibiotics is represented by the two-component antimicrobial peptides that exhibit much higher biological activity in synergy. At the present, this group includes staphylococcin C55 from *Staphylococcus aureus* C55 (*2*), lacticin 3147, Ltnα and Ltnβ from *Lactococcus lactis* DPC3147 (*3*), plantaricin W from *Lactobacillus plantarum* (*4*), SmbA and SmbB from *Streptococcus* mutants GS5 (*5*), BHT-A from *Streptococcus rattus* BHT (*6*), and haloduracin, Halα, and Halβ from *Bacillus halodurans* C-125 (*7*). The majority of known two-component lantibiotic systems were characterized only at the level of precursor nucleotide sequences. Up to now, chemical structures of mature two-component lantibiotics with characterization of post-translational modifications were reported only for two of them: lacticin 3147, Ltnα and Ltnβ (*8*), and haloduracin, Halα and Halβ (*9*). Sequence comparison in the NCBI database showed that two strains of *Bacillus lichenifirmis*, ATTC14580 and DSM13, contain a putative two-component lantibiotic gene cluster which comprises two structural genes (ATTC14580: *bliA1* and *bliA2* (*10*); DSM13: *licA1* and *licA2* (*11*)). The corresponding two-component peptides (Bliα, Bliβ, Licα, and Licβ) were only partially characterized, thus awaiting detailed biochemical and structural investigations (*10*, *11*).

In this study, we isolated a synergetic lantibiotic pair, Lchα (3249.51 Da) and Lchβ (3019.36 Da), termed lichenicidin VK21, from the producer strain *Bacillus licheniformis* VK21. A lantibiotic cluster of *Bacillus licheniformis* VK21 genome which comprises the structural genes, *lchA1* and *lchA2*, encoding the lichenicidin VK21 precursors, as well as the gene of a modifying

[†]This work was supported by the Federal Target Program "Scientific and Science-Educational Personnel of Innovative Russia" [project NK-602P/19].

[‡]The peptides sequence data reported in this article have been deposited in the UniProt knowledgebase under the accession numbers P86475 for Lchα and P86476 for Lchβ. The NMR assignments of Lchα and Lchβ have been deposited in the BMRB as entries 16707 and 16709, respectively. Spatial structures have been deposited in PDB under the record numbers 2KTN for Lchα and 2KTO for Lchβ. The nucleotide sequence of the lichenicidin VK21 lantibiotic cluster have been deposited in GenBank under the record GU949560.

*To whom correspondence should be addressed. Phone: +7-(495)-336-44-44. Fax +7-(495)-336-43-33. E-mail: ovch@ibch.ru.

[1]Abbreviations: CFU, colony-forming units; CID, collision-induced dissociation; Dha, 2,3-didehydroalanine; Dhb, 2,3-didehydrobutyrine; FT-ICR MS, Fourier transform ion cyclotron resonance mass spectrometry; Lan, lanthionine; MBC, minimal bactericidal concentration; MeLan, 3-methyllanthionine; MIC, minimal inhibitory concentration; Mrs, mersacidin; NOE, nuclear Overhauser effect; Nis, nisin; OBu, 2-oxobutyryl; rmsd, root-mean-square deviation; SIM, selected ion monitoring.

 Published on Web 06/25/2010

enzyme *lchM1*, was amplified and sequenced. Chemical and spatial structures of the mature peptides were determined by NMR spectroscopy. It was shown that Lchα and Lch*β* interact synergistically to possess antibiotic activity against Gram-positive bacteria in the nanomolar concentration range, though the individual peptides were shown to be active at micromolar concentrations. Thus, lichenicidin VK21, Lchα and Lch*β*, was found to be a novel two-component lantibiotic which has the potential in the development of new drugs.

MATERIALS AND METHODS

Bacterial Culture. *Bacillus licheniformis* VK21 was from the Branch of Shemyakin and Ovchinnikov Institute of Bioorganic Chemistry (Pushchino, Russia). The culture was grown for 16 h in LB-agar at 45 °C for 24 h and then was diluted with 10 mL of C2Mn medium (0.15% casamino acids, 0.02% KCl, 0.3% K_2HPO_4, 0.1% KH_2PO_4, 0.02% $MgSO_4 \times 7H_2O$, 0.001% $MnSO_4 \times 5H_2O$, 0.4% sucrose, w/v, pH 7.3). Aliquots of the obtained cell suspension (1.5 mL) were placed in 700-mL flasks filled with 150 mL of C_2Mn medium each. The flasks were incubated at 45 °C for 6 h in an orbital shaker at 200 r/min to a final optical density at 620 nm of 1.5 (a stationary-phase culture).

Lantibiotics Purification. The *Bacillus licheniformis* VK21 culture was centrifuged at 8000*g* for 50 min. The supernatant was 20-fold concentrated by rotary evaporation. Two-fold volume of acetone was added to the obtained solution, and the precipitate was removed by centrifugation at 8000*g* for 40 min. The supernatant was collected and dried using a rotary evaporator and dissolved in 50 mL of water. After extraction with equal an volume of *n*-butanol, the organic phase was dried and then dissolved in 50 mL of buffer A_1 (30 mM ammonium acetate, pH 5.6, 30% v/v acetonitrile) and applied to a Silasorb C_8 column pre-equilibrated with buffer A_1. After washing, the column with 100 mL of buffer A_1, initial separation was developed in 50 mL of buffer solution B_1 (30 mM ammonium acetate, pH 5.6, 80% v/v acetonitrile) at a flow rate of 2 mL/min. The collected eluent was diluted with 30 mM ammonium acetate, pH 5.6, to reach 30% v/v acetonitrile concentration, and applied to a Diasorb-130C_8T column. After washing the column with buffer A_1, further separation was achieved in a linear gradient of buffer B_1 from 0 to 100% for 95 min (1.05%·min^{-1}) at a flow rate of 2 mL/min. Fractions with peak optical density at 214 nm were collected. Aliquots of the fractions were tested for antimicrobial activity against *M. luteus* and *B. megaterium*. Active fractions were purified by RP-HPLC on a Diaspher-110-C_4 column pre-equilibrated with solution A_2 (5% acetonitrile and 60% methanol, v/v) in a linear gradient of solution B_2 (35% acetonitrile and 60% methanol, v/v) from 0 to 100% for 40 min (2.5%·min^{-1}) at a flow rate of 0.5 mL/min.

Purification of Genome DNA. *Bacillus licheniformis* VK21 was grown overnight at 45 °C in C_2Mn medium (0.15% casamino acids, 0.02% KCl, 0.3% K_2HPO_4, 0.1% KH_2PO_4, 0.02% $MgSO_4 \times 7H_2O$, 0.001% $MnSO_4 \times 5H_2O$, and 0.4% sucrose, w/v, pH 7.3). Cells were pelleted via centrifugation at 3000*g* for 5 min, washed with 0.85% NaCl and resuspended in TEN buffer (0.15 M NaCl, 0.1 M Tris-HCl, and 0.01 M EDTA, pH 8.0) with lysozyme (4 mg/mL) at a ratio of 2:5 (v/v). After incubation at 37 °C for 45 min, 8.5% SDS was added at a ratio of 1:6 (v/v), and the suspension was heated to 75 °C for 30 min. Potassium acetate (5 M, pH 5.2) was added to the obtained cell lysate at a ratio of 1:2.5 (v/v), the mixture was incubated at 4 °C for 20 min, and centrifuged at 10000*g* for 5 min, and the supernatant was decanted. The precipitate containing genome DNA was dissolved in TE buffer (10 mM Tris-HCl, 1 mM EDTA, pH 8.0). Genome DNA was purified by standard methods of phenol−chloroform extraction and isopropanol precipitation (*12*)

Genes Sequence Analysis. Genes sequencing strategy was based upon the total genome sequence of *Bacillus licheniformis* strain ATCC 14580 that contains a cluster of *lan* genes (*13*). Two sense (internal, 5′-GAAGAAAACCATCCCTGCAA-3′, and external, 5′-GCTCATTCTCGTCATCCCTT-3′) and two antisense (internal, 5′-GCGCTCGAGTTAAAACACGTTT-TCTCTTT-3′, and external, 5′- GCGCATTTGGATGAAG-GTCT-3′) primers flanking the region of interest were synthesized to improve chances of successful amplification in case of mutation in the annealing site in the *Bacillus licheniformis* strain VK21 genome. The reaction was performed using Taq Advantage II polymerase mix (Clontech). The PCR product of about 3900 bp in length containing *lchA1, lchA2*, and *lchM1* genes was ligated into pGEM-T vector (Promega), which was then used for transformation of *E. coli* DH-10B competent cells. The plasmid DNA was purified using a plasmid miniprep kit (Zymo Research). Nucleotide sequencing analysis was performed using ABI PRISM 3730 automatic sequencer with a ABI PRISM BigDye Terminator v. 3.1 reaction kit (Applied Biosystems, USA).

NMR Spectroscopy and Spatial Structure Calculation. NMR spectra were acquired using Bruker 700 MHz Avance spectrometer equipped with a triple resonance (^{1}H, ^{13}C, and ^{15}N) TCI cryoprobe. All measurements were done for 0.5 mM peptide samples in d_3-methanol at 27 °C and pH 3.5 (uncorrected pH-meter readings). ^{1}H Chemical shifts were referenced relative to residual CD_2H signal of methanol at 3.31 ppm. The ^{13}C chemical shifts were referenced indirectly relative to TMS. Spatial structure calculation was performed using the simulated annealing/molecular dynamics protocol as implemented in the CYANA program, version 2.1 (*14*). Upper interproton distance constraints were derived from NOESY (τ_m = 200 ms) cross-peaks via a $1/r^6$ calibration. The torsion angle constraints were obtained from $^3J_{HNH}{}^{\alpha}$ coupling constants which were determined from line shape analysis of NOESY cross-peaks in the program Mathematica (Wolfram research). Closure and proper geometry of Lan and MeLan thioether bridges were forced during calculation using two upper and one lower distance constraints for each bridge. Analysis of preliminary structures allows one to introduce additional constraints. The lower distance constraints (3.0 Å), based on the expected cross-peaks but not present in the NOESY spectra, were introduced. Hydrogen bonds observed in more than 50% of preliminary structures (3 bonds for Lchα and 18 bonds for Lch*β*) were also restrained to enforce better structural convergence during the final stage of calculation. The D-enantiomeric form of AlaS and AbuS residues that originated from Ser and Thr by post-translational modifications and participated in the formation of Lan and MeLan bridges was accounted for during structure calculation. The corresponding D-AlaS and D-AbuS residues were introduced in the CYANA library. The D-enantiomeric form for other residues in Lchα and Lch*β* was found to be incompatible with obtained NOE intensities and $^3J_{HNH}{}^{\alpha}$ couplings (data not shown). The cis-configuration of the $C^{\alpha}-C^{\beta}$ double bond in Dhb residues (Z isomer) was verified by the observation of strong intraresidual NOE contacts between $^1H^N$ and methyl H^{γ} protons.

Mass Spectrometry. High-resolution FT-ICR mass spectra were measured on a 7-T Finnigan LTQ FT spectrometer

equipped with an Ion Max electrospray ion source (Thermo). FTMS data were acquired in the positive ion mode with resolution R = 100,000 (full scan) and R = 400,000 (selected ion monitoring scan, SIM) at m/z 400. For external mass calibration, LTQ FT tuning mix was used to give mass error <2 ppm. Tandem FT-ICR MS/MS data were obtained using collision-induced dissociation (CID).

Antibacterial Activity Assay. The bacteria *Bacillus subtilis*, strain L1, *Rhodococcus* sp., strain SS2, *Micrococcus luteus*, strain B1314, *Pseudomonas aeruginosa*, strain PAO1, and *Pseudomonas putida*, strain I-97, were obtained from Institute of Biochemistry and Physiology of Microorganisms (Pushchino, Russia). The strain *Escherichia coli* C600 was obtained from Branch of Shemyakin and Ovchinnikov Institute of Bioorganic Chemistry (Pushchino, Russia). The strain *Bacillus megaterium* VKM41 was obtained from All-Russian Collection of Microorganisms (Pushchino, Russia). The bacterium *Staphylococcus aureus*, strain 209p, was obtained from Kuban State Medical Academy (Krasnodar, Russia). The bacteria *Bacillus pumilus*, strain 2001, *Bacillus globigii*, strain I, *Bacillus amyloliquefaciens*, strain I, *Mycobacterium smegmatis*, strain 1171, and *Mycobacterium phlei*, strain 1291 were obtained from Afanasiev Research Institute of Fur-Bearing Animals and Rabbits (Rodniki, Moscow region, Russia).

Antimicrobial activities of purified peptides toward Gram-positive and Gram-negative bacteria were measured in radial diffusion assays by the gel overlay techniques as described previously (*15*) and by microspectrophotometry using 96-well microplates as described (*16*). Wells were filled with 20% methanol solution (10 μL) of individual peptides (or their mixture at different ratios) in serial dilutions and mixed with 110 μL of exponential test cultures (2×10^8 CFU mL^{-1} on the average), 10-fold diluted by 1/2LB (or 2LB, 1% sucrose for *Micrococcus luteus*). Bacterial growth was evaluated by measuring the culture OD_{620} using a microplate reader Multiscan EX (Thermo). Optical density was recorded during 5 h. The plates were incubated at 30 °C. IC_{50} was defined as the concentration of peptide which was needed to inhibit test culture growth by half (50%). MIC was defined as the lowest concentration of peptide that prevented visible bacterial growth after overnight incubation. MBC was determined by plating 110 μL of broth from each well, where there is no visible test culture growth in the MIC experiment, on LB-agar plates and incubated overnight. MBC was defined as the lowest peptide concentration that prevented bacteria growth on the agar surface after incubation overnight and resulted in >99.9% CFU reduction by comparison with controls (*17*).

RESULTS

Sequencing of the Lantibiotic Cluster of the B. licheniformis VK21 Genome. Using primers for the *Bacillus licheniformis* ATCC14580 lantibiotic cluster (GenBank record CP000002), we amplified and sequenced a part of the *Bacillus licheniformis* VK21 genome containing the genes of two lantibiotic precursors (*lchA1* and *lchA2*) and a modifying enzyme (*lchM1*). The gene located downstream of *lchA1* is referred to as *lchM1* in this work (Figure 1A). Comparison of the corresponding nucleotide sequences showed that the structural genes of lantibiotic precursors are completely identical, while the *lchM1* gene contains 9 point mutations, and 5 of them lead to amino acid substitutions (Table S1, Supporting Information). Sequencing of the lantibiotic cluster of the *B. licheniformis* VK21 genome provides structures of the LchA1 and LchA2 prepeptides (Figures 1B and C), the precursors of the lantibiotics Lchα and Lchβ.

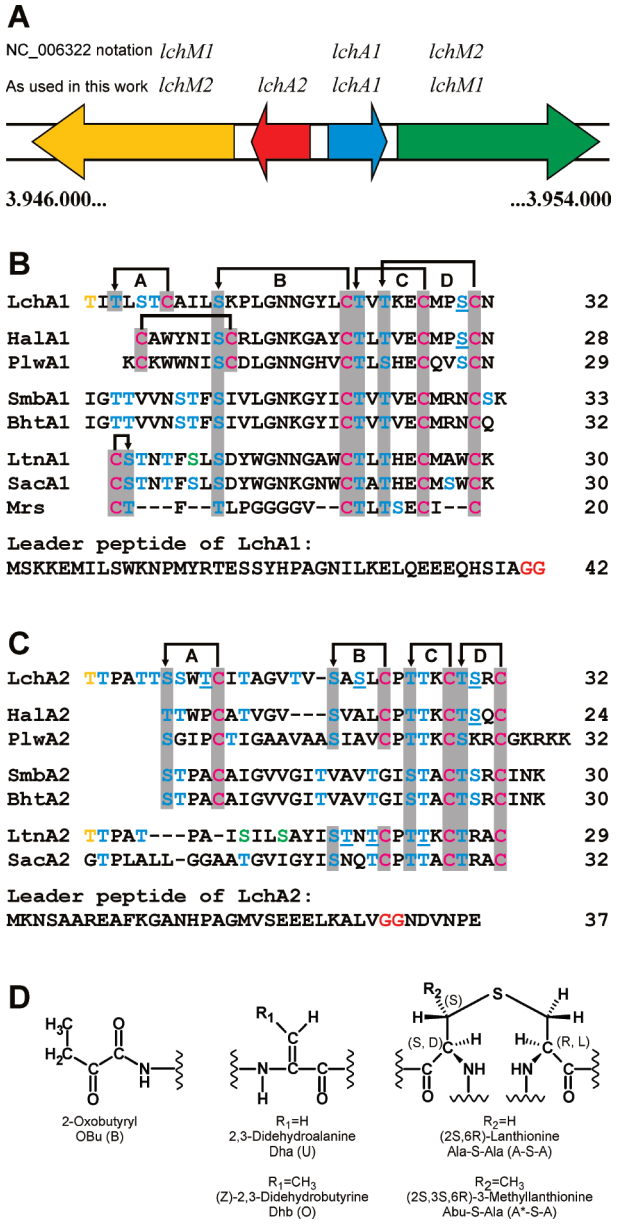

FIGURE 1: Lichenicidin VK21 gene cluster and amino acid alignment of LchA1 and LchA2 with other lantibiotics propeptides. (A) The lichenicidin VK21 gene cluster. The nucleotide numbering is given accordingly to GenBank record CP000002. (B,C) LchA1 and LchA2 in comparison with other lantibiotic propeptides: haloduracin, HalA1 and HalA2 (*7*); plantaricin W, PlwA1 (AAG02567) and PlwA2 (AAG02566); SmbA1 (annotated as SmbB, BAD72777) and SmbA2 (annotated as SmbA, BAD72776); Bht, BhtA1 (AAZ76603) and BhtA2 (AAZ76602); lacticin 3147, LtnA1 (O87236) and LtnA2 (O87237); staphylococcin C55, SacA1 (BAB78438) and SacA2 (BAB78439); mersacidin, Mrs (CAA87640). A GenBank accession number is given in parentheses for each sequence. Ser/Thr residues, post-translationally modified to D-Ala/Obu, are shown in green/yellow. Other Ser/Thr residues are marked in cyan, and unmodified ones are underlined. Cys residues are shown in magenta. Thioether and disulfide bonds are indicated with arrows and are boxed in gray. Thioether bridging rings in the mature Lchα and Lchβ are marked with the capital letters A, B, C, and D. The most probable LchT protease cleavage site sequences are shown in red. The chemical structures of post-translationally modified amino acids are shown in panel D.

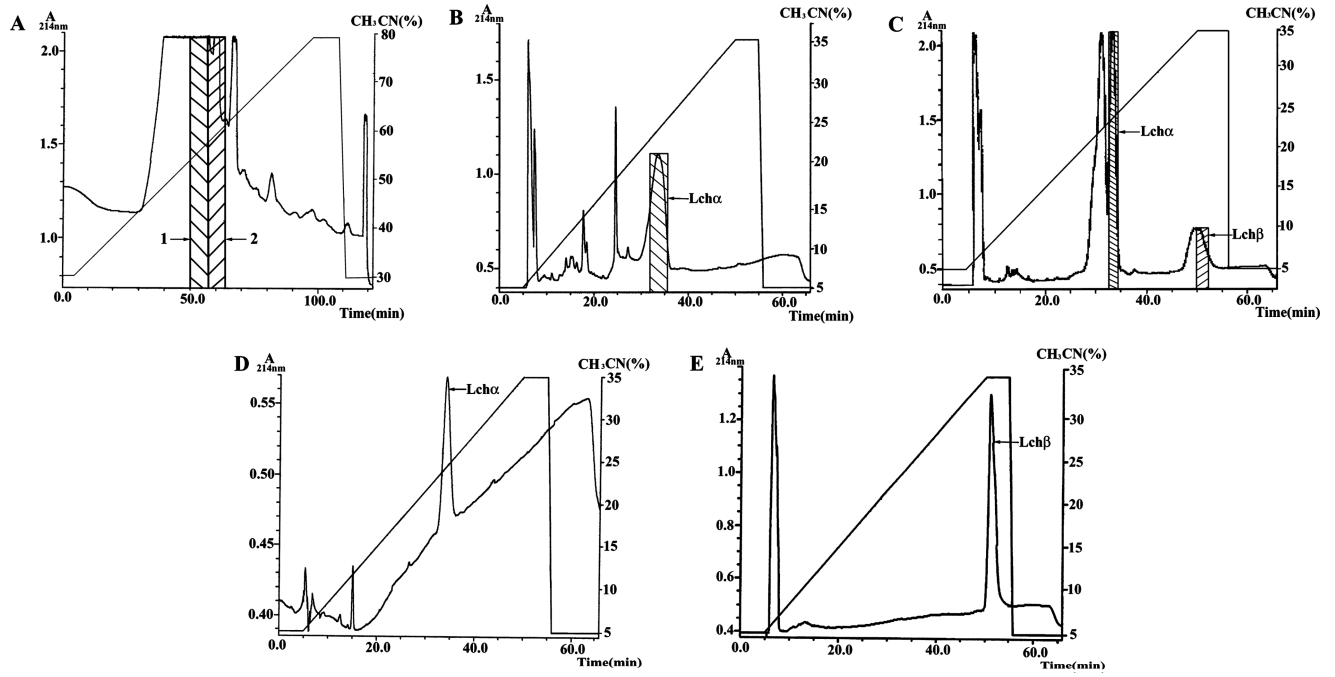

FIGURE 2: HPLC purification of Lchα and Lchβ. (A) Elution profile of the first-round purification of a crude extract of lichenicidin VK21 by RP-HPLC on to a Diasorb-130C8T column in a linear gradient of acetonitrile from 30 to 80%. Fractions 1 and 2, shown by hatching, were biologically active against *M. luteus* and *B. megaterium*. (B,C) Elution profiles of the second-round purification using pooled fractions 1 (B) and 2 (C) from the first pass as starting material. Purification by RP-HPLC on a Diaspher-110-C4 column in a linear gradient of acetonitrile from 5 to 35%. Active fractions containing Lchα and Lchβ are shown by hatching. (D,E) RP-HPLC of the individual peptides Lchα and Lchβ, respectively.

Isolation and Purification of Lchα and Lchβ. To identify and characterize novel peptide lantibiotics, we isolated them from the *Bacillus licheniformis* VK21 culture as described above. Figure 2 summarizes the results of the HPLC purification of Lchα and Lchβ. RP-HPLC on a Diasorb-130C_8T column in a linear gradient of acetonitrile from 30 to 80% v/v allowed us to identify two biologically active fractions (Figure 2A). Each active fraction was purified by RP-HPLC on a Diaspher-110-C_4 column in a linear gradient of acetonitrile from 5 to 35% v/v (Figures 2B and C). The RP-HPLC purification procedure resulted in purification to homogeneity of two individual peptides, named Lchα and Lchβ (Figures 2D and E). FT-ICR mass spectrometry of the purified mature peptides revealed monoisotopic molecular masses of 3249.51 Da for Lchα and 3019.36 Da for Lchβ (Figure S1, Supporting Information). It is noteworthy that we isolated some premature forms of Lchα (MW of ~3268 Da) and Lchβ (MW of ~3038 Da) displaying biological activity, but the completely post-translationally modified peptides Lchα and Lchβ were the most active. The isolated peptides Lchα and Lchβ were subsequently subjected to detailed structural and biochemical characterization.

Antimicrobial Activity of Lichenicidin VK21. Biological activities of the purified Lchα and Lchβ peptides were preliminary measured in a radial diffusion assay by the gel overlay techniques. Samples were tested for antimicrobial activity against a battery of Gram-positive and Gram-negative bacteria (see Materials and Methods). Both Lchα and Lchβ were active against all the tested Gram-positive bacteria: *B. subtilis*, strain L1, *Rhodococcus* sp., strain SS2, *M. luteus*, strain B1314, *B. megaterium*, strain VKM41, *S. aureus*, strain 209p, *B. pumilus*, strain 2001, *B. globigii*, strain I, *B. amyloliquefaciens*, strain I, *M. smegmatis*, strain 1171, and *M. phlei*, strain 1291. The ability of the Lchα + Lchβ mixture at a molar ratio of 1:1 to inhibit growth of the most sensitive test-microorganisms (*M. luteus*, strain B1314, Figure 3A; *B. megaterium*, strain VKM41, Figure 3B; *Rhodococcus* sp., strain SS2, Figure 3C; *B. subtilis*, strain L1, Figure 3D; and *S. aureus*, strain 209p, Figure 3E) was examined at different concentrations by the 96-well microplate method. Comparison of antibiotic effects of individual peptides and their equimolar mixture against Gram-positive bacteria are shown in Table 1. Although antimicrobial effects of individual peptides Lchα and Lchβ were within the micromolar concentration range, biological activity of their mixture at a ratio of 1:1 was much higher than the sum of their individual contributions. Thus, Lchα and Lchβ interact synergistically to possess antibiotic activity against Gram-positive bacteria within the nanomolar concentration range. Neither the individual peptides nor their mixture is active against Gram-negative bacteria *P. aeruginosa*, strain PAO1, *P. putida*, strain I-97, and *E. coli*, strain C600, in the maximal tested concentration (17-fold higher than the maximal IC_{50} for Gram-positive bacteria). Hereafter, the antimicrobial activity of lichenicidin VK21 was studied by the 96-well microplate assay at varying Lchα/Lchβ molar ratios. *B. megaterium*, strain VKM41, was used as the test microorganism, being one of the most sensitive to lichenicidin VK21. The ability of Lchα and Lchβ to inhibit growth of the test microorganism was examined at different concentrations and ratios of the individual peptides. The diagram (Figure 3F) indicates that lichenicidin VK21 displays the highest activity at the 1:1 molar ratio of Lchα and Lchβ.

Structure of the Mature Peptides Lchα and Lchβ. To determine the complete structure of the mature peptides including the sites of post-translational modification (dehydration of Ser and Thr, cyclization, proteolytic digestion, etc.), the methods of NMR spectroscopy were employed (*18*). Each peptide was studied in a solution of perdeuterated methanol (CD_3OH) where both Lchα and Lchβ are soluble at millimolar concentrations. Moderately acidic conditions (pH 3.5) were used to decrease broadening of $^1H^N$ signals associated with solvent exchange. To identify the spin systems of amino acid residues and their sequential

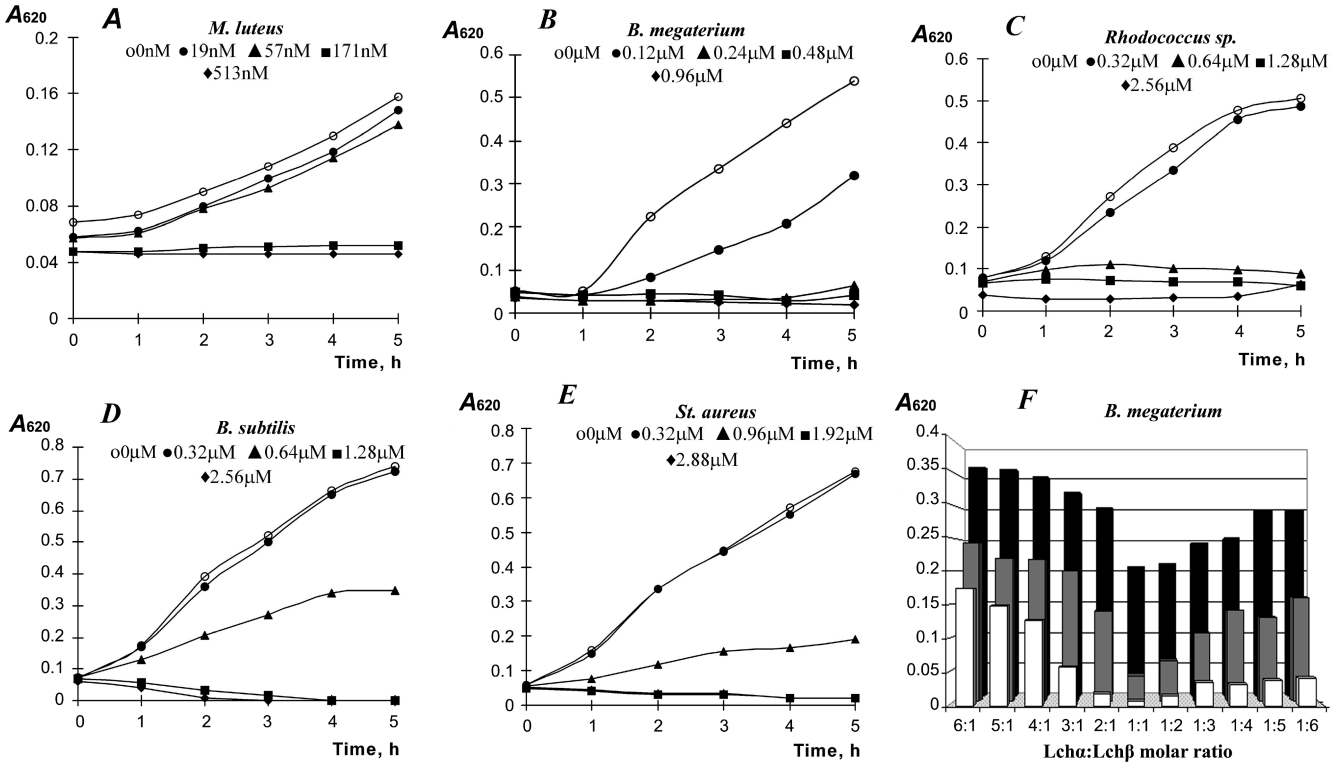

FIGURE 3: (A−E) Antimicrobial activity of the Lchα and Lchβ mixture (at a 1:1 ratio) against Gram-positive bacteria at different concentrations (●, ▲, ■, ♦); (○) control without the peptides. (F) Effects of the Lchα and Lchβ mixture on *Bacillus megaterium* VKM41 growth at varying ratios of the peptides and different total concentrations shown in white (0.36 μM), gray (0.24 μM), and black (0.12 μM).

Table 1: Effects of Lichenicidin VK21 and Individual Peptides Lchα and Lchβ against Gram-Positive Bacteria

peptides	concentration, μM	*B. megaterium*	*B. subtilis*	*M. luteus*	*Rhodococcus* sp.	*S. aureus*
Lchα	IC_{50}	1.8	9	1.2	9	3.1
	MIC	7.2	15	>4.8	>15	18.4
	MBC	10.8	>36	nd[a]	nd	>46.1
	MBC/MIC	1.5	nd	nd	nd	>2.5
Lchβ	IC_{50}	2	30	2.6	16.6	20
	MIC	12	>50	>5.3	>16.6	50
	MBC	>12	nd	nd	nd	nd
	MBC/MIC	nd	nd	nd	nd	nd
Lchα + Lchβ	IC_{50}	0.12	0.64	0.09	0.64	0.64
	MIC	0.48	0.96	0.17	>2.56	0.96
	MBC	0.96	3.84	1.92	nd	>4.8
	MBC/MIC	2	4	11	nd	>5

[a]nd. not determined.

connectivities, a standard combination of 2D TOCSY and NOESY spectra (*19*) was used (Figure S2, Supporting Information). Assignment of spin systems to defined residue types was significantly facilitated by the information about ^{13}C chemical shifts obtained from 2D ^{13}C-HSQC spectra measured at natural isotopic abundance. In addition, analysis of the aromatic region of HSQC spectra provided straightforward identification of dehydrated residues (Dha and Dhb) in both peptides (Figure 4A,B). The bridging patterns of Lan and MeLan residues were deduced from characteristic $^1H^{\alpha}$-$^1H^{\beta}$, $^1H^{\beta}$-$^1H^{\beta}$, and $^1H^{\beta}$-$^1H^{\gamma}$ NOE connectivities (Figure S3, Supporting Information). In some cases, the obtained sequential NMR data were incomplete, thus requiring comparison with genomic data for the determination of the full chemical structure of Lchα and Lchβ.

Three sequence fragments were identified in the NMR spectra of Lchα (Figure 4E, underlined). The first of them, Ile2-Leu10 (numbers are given in accordance with the mature lantibiotic sequence), includes one MeLan (Abu3-S-Ala7) and two dehydrated (Dha5, Dhb6) residues. The second fragment, AlaS11-Asn17, includes AlaS of Lan residue. The third identified fragment, Gly18-Asn32, involves AlaS21 of Lan, two MeLan residues (Abu22-S-Ala27, Abu24-S-Ala31), and unmodified Ser30 residue. No other spin systems corresponding to unmodified Ser or Thr residues were detected in the ^1H and ^{13}C NMR spectra of the mature Lchα. Comparison of the structure of LchA1 prepeptide with the NMR derived sequence fragments allowed us to locate them sequentially from the N- to C-terminus of the mature peptide and provided the complete chemical

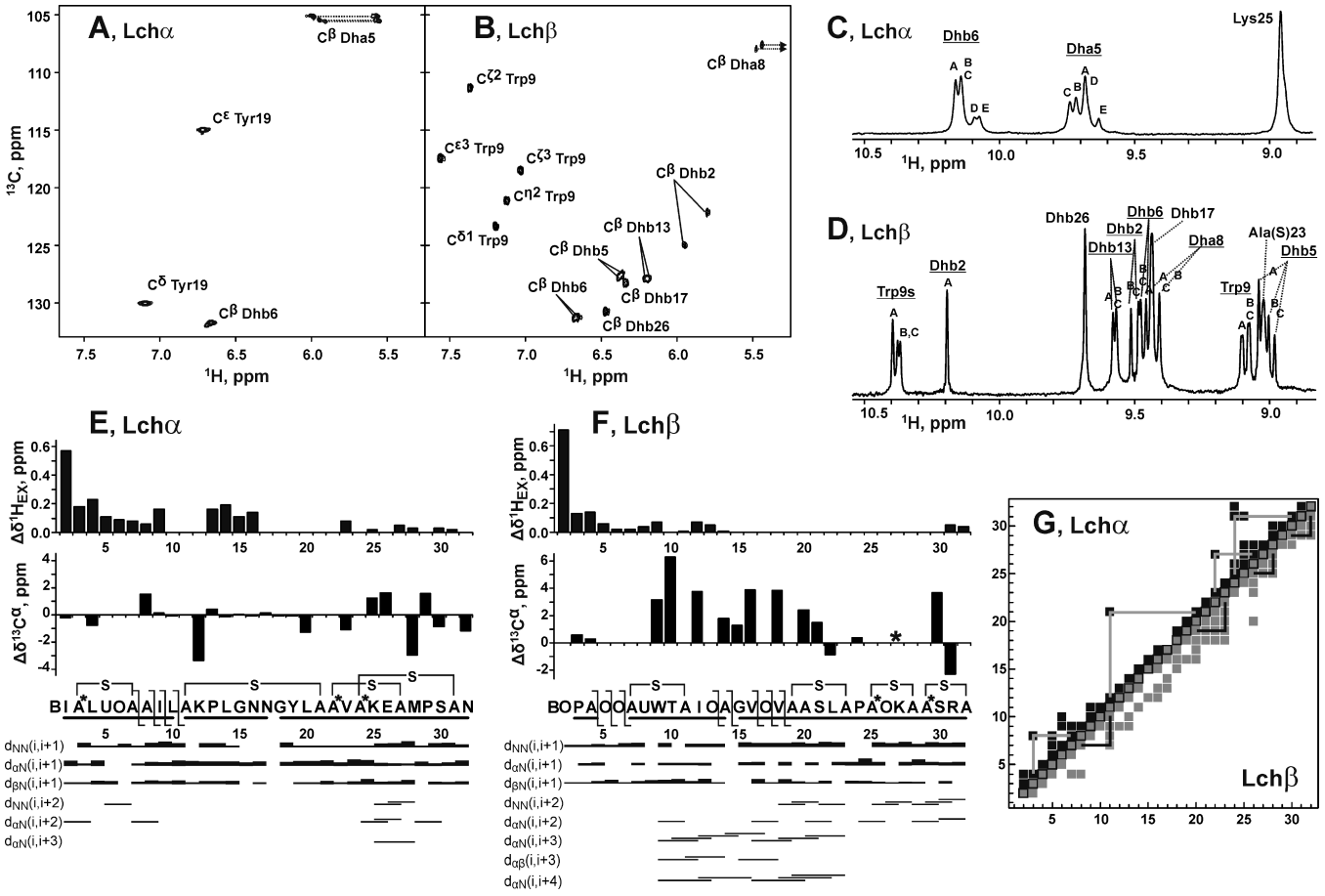

FIGURE 4: NMR and MS data define the primary structure of Lchα and Lch*β*. (A,B) Aromatic regions of 2D ^{13}C-HSQC spectra provide the identification of Dha and Dhb residues. (C,D) Downfield amide region of 1D ^{1}H spectra shoving multiple conformations of Lchα and Lch*β* in methanol solution (pH 3.5, 27 °C). The obtained resonance assignment is shown, the signals originating from different conformational states of the peptides are marked by capital letters (A, B, C, D, and E) and (A, B, and C) for Lchα and Lch*β*, respectively. In each case, the major conformational state is designated as A. (E,F) The NOE connectivities, $^{13}C^{\alpha}$ secondary chemical shifts ($\Delta\delta^{13}C^{\alpha}$), differences of ^{1}H chemical shifts between different conformational states of the peptides ($\Delta\delta^{1}H_{EX}$), and fragmentation observed in tandem MS/MS (vertical S-shaped lines) are shown versus proposed amino acid sequences of Lchα and Lch*β*. The NMR derived sequence fragments are underlined. The NOE connectivities are denoted as usual, except that N denotes amide protons or H^{δ} protons for Pro residues. The widths of the bars correspond to the relative intensity of the cross-peak in the 200 ms NOESY spectrum. The amino acid sequences are given in the one letter code format, where 2-oxobutyryl, 2,3-didehydroalanine, 2,3-didehydrobutyrine, lanthionine, and methyllanthionine are abbreviated as B, U, O, A-S-A, and A*-S-A, respectively. (G) NOE contact maps of Lchα and Lch*β*. Each square corresponds to at least one observed NOE between the two corresponding residues. The residues forming the thioether bridge are connected by lines.

structure of Lchα (Figures 4E and 5A). An attempt to obtain unequivocal sequential connectivities at Leu10-AlaS11 and Asn17-Gly18 sites by NMR methods failed due to the degeneracy of $^{1}H^{N}$ chemical shifts (Table S2, Supporting Information).

Similarly, two large sequence fragments were identified in the NMR spectra of Lch*β* (Figure 4F, underlined). The first of them, AlaS7-Ala14, involved one Lan (Ala7-S-Ala11), two dehydrated residues (Dha8, Dhb13), and one unmodified Thr10 residue. The second fragment, Gly15-AlaS32, contained one Lan (Ala19-S-Ala23), two MeLan (Abu25-S-Ala28, Abu29-S-Ala32), two dehydrated (Dhb17, Dhb26), and two unmodified Ser (Ser21, Ser30) residues. No other unmodified Ser and Thr residues were detected in the mature Lch*β*. At the same time, analysis of the Lch*β* NMR spectra revealed the presence of three additional Dhb residues and Pro3-Ala4 dipeptide fragment. Comparison of the NMR derived structural data with the sequence of LchA2 prepeptide provided unambiguous chemical structure of the mature lantibiotic Lch*β* (Figures 4F and 5B). Combination of the obtained NMR and genomic data disprove the formation of disulfide bonds and conversion of Ser to D-Ala during the maturation of Lchα and Lch*β* peptides.

Observation of $^{1}H^{N}$ signals for Ile2 and Dhb2 residues in the NMR spectra of Lchα and Lch*β*, respectively, implies the presence of blocking groups at the N-termini of both peptides. This conclusion is also supported by the inability to sequence both peptides by Edman degradation. Inspection of the prepeptide sequences indicated that both LchA1 and LchA2 contain Thr residues in a position that precedes the lantibiotic encoding sequences. Most probably, these N-terminal Thr residues are initially dehydrated to Dhb and after that undergo spontaneous hydrolysis to 2-oxobutyryl groups (OBu) during the maturation of Lchα and Lch*β*. The presence of OBu residues in Lchα and Lch*β* was supported by an analysis of ^{1}H and ^{13}C NMR spectra, where the spin system corresponding to CH_3-CH_2− fragment with characteristic chemical shifts was observed (Tables S2 and S3, Supporting Information). Interestingly, there were no NOE contacts between OBu and other residues of the peptides in the NMR spectra, thus indicating increased intramolecular mobility within the N-terminal fragments of both peptides.

The determined chemical structures of Lchα and Lch*β* are schematically presented in Figures 5A and 5B. These structures are supported by the results of high-resolution FT-ICR MS

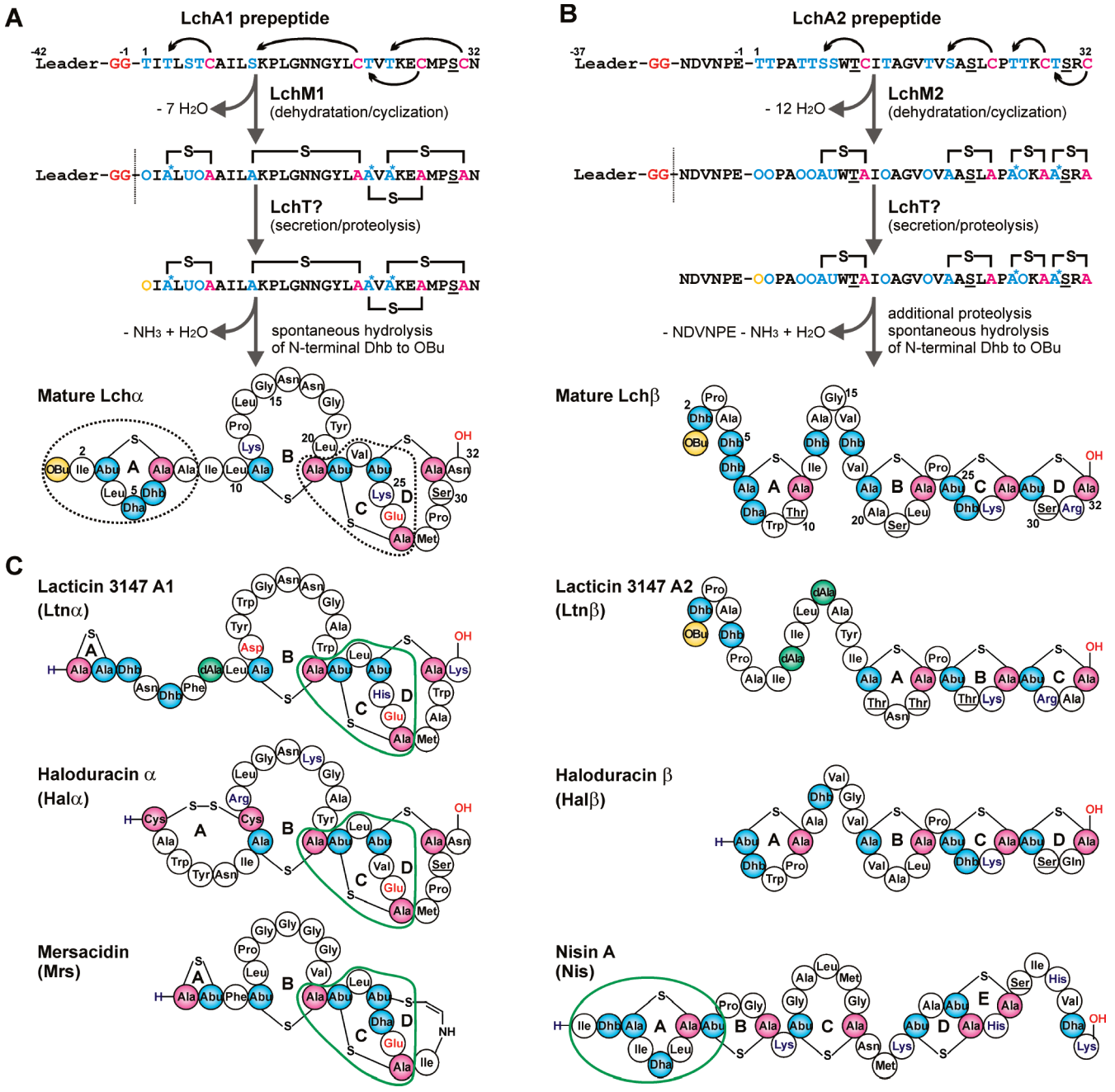

FIGURE 5: Comparison of Lchα and Lch*β* structures with other lantibiotics. (A,B) Proposed mechanism of Lchα and Lch*β* maturation and their primary structures. The amino acid sequences are given in the one letter code format as described in Figure 4. The residues are color coded as indicated in Figure 1. (C) Primary structures of lacticin 3147, haloduracin, mersacidin, and nisin A. The lipid II binding domains are circled. The positively and negatively charged residues are shown in blue and red, respectively.

analysis (Figure S1, Supporting Information). The experimentally determined molecular masses of Lchα (3249.51 Da) and Lch*β* (3019.36 Da) matched the calculated masses of the proposed structures (3249.515 and 3019.360 Da, respectively) within the experimental error (0.01 Da). The proposed chemical structures are also consistent with results of tandem FT-ICR MS/MS data (Figures 4E,F, vertical S-shaped lines, and Figure S1, Supporting Information).

Spatial Structure and Dynamics of Lchα and Lchβ in Methanol Solution. One of the most sticking features of the Lchα and Lch*β* NMR spectra is the presence of considerable signal doubling (Figure 4C,D). Five and three sets of NMR signals with relative abundances ~40:20:20:10:10 and ~50:25:25 were observed for Lchα and Lch*β*, respectively. The largest (up to 0.6 ppm) differences of ^{1}H chemical shifts ($\Delta\delta^1H_{EX}$) between corresponding signals from different sets were observed in both peptides for the N-terminal residues (Figures 4E,F, upper panels). In addition, substantial signal doubling (with $\Delta\delta^1H_{EX}$ up to 0.2 ppm) was detected for Pro13-Asn16 residues of Lchα. The C-terminal fragments of both peptides also demonstrate the presence of signal doubling, but the associated chemical shift differences were relatively small ($\Delta\delta^1H_{EX}$ less than 0.1 ppm).

In general, the observed signal doubling can be originated either by the sample inhomogeneity or conformational exchange process(es) going slow in an NMR time scale. The results of RP-HPLC (Figure 2) and FT-ICR MS analyses (Figure S1, Supporting Information) proved the purity of the Lchα and Lch*β* samples. Moreover, no signals of unassigned Thr or Dhb residues

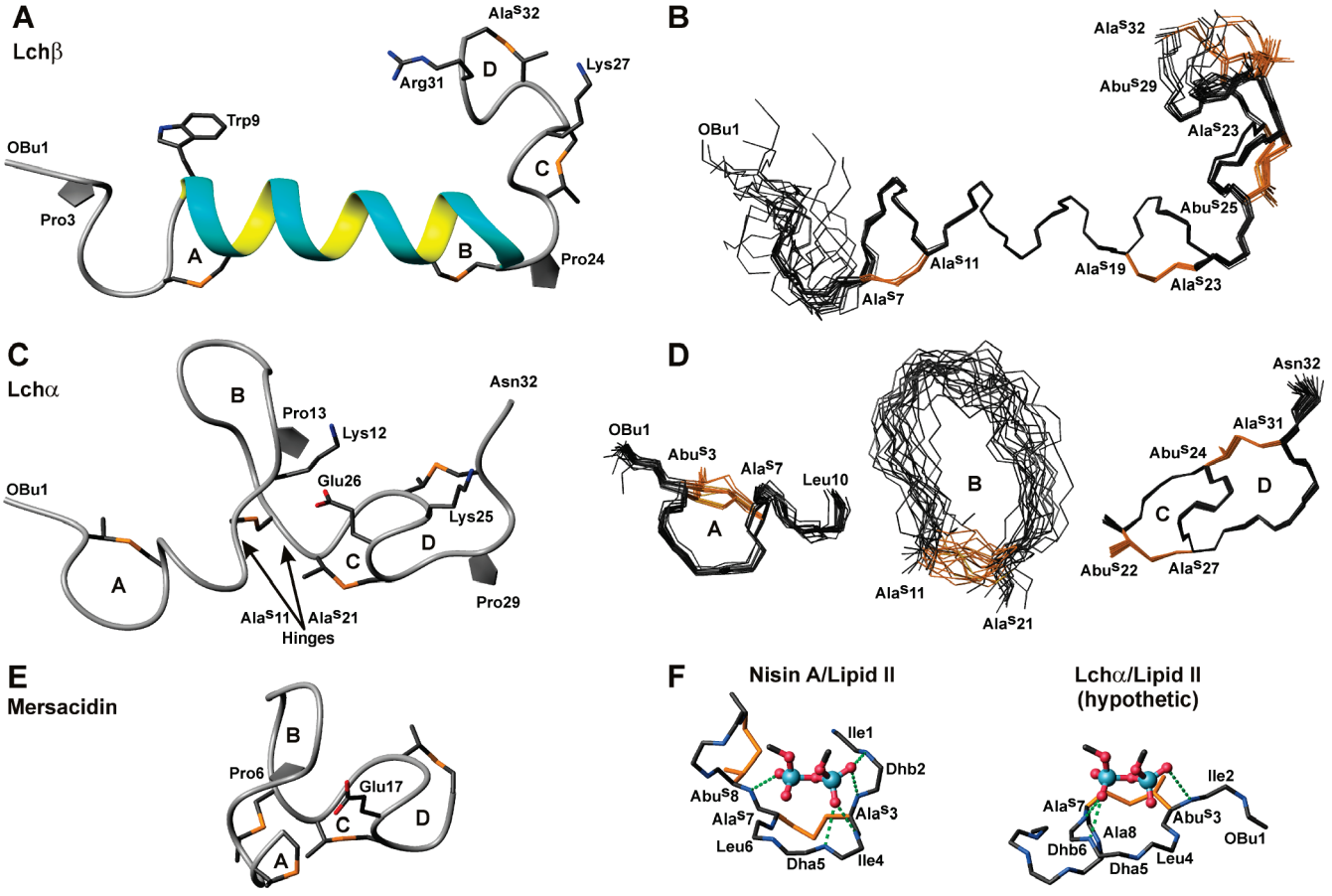

FIGURE 6: Spatial structure of Lchα and Lch*β* in comparison with mersacidin and nisin. (A,B,C,D) The calculated structural ensembles for Lch*β* and Lchα together with representative conformers in ribbon representation. The 20 selected structures of Lch*β* (panel B) are superimposed by the central helical domain (AlaS7−Pro24). The superimposition of 20 selected structures of Lchα (panel D) was done on the level of individual domains. In panels A and C, Lan, MeLan, Glu, Arg, Lys, and Trp residues are in stick representation, and Pro residues are shown by planes. In panels B and D, Lan and MeLan residues are in yellow. (E) The crystal structure of mersacidin (PDB 1QOW) (*33*). (F) Structure of the nisin/lipid II complex determined by NMR spectroscopy (PDB 1WCO) (*26*) and the model of the Lchα/lipid II complex obtained by superimposition of the backbone atoms of nisin and Lchα in the region of thioether ring A. The N-terminal fragments of both peptides are shown with Lan and MeLan residues in yellow. The pyrophosphate moiety of lipid II is in ball-and-stick representation. The hydrogen bonds between backbone amides and pyrophosphate oxygenes are shown by green dashed lines. The figure was prepared using the MOLMOL program (*35*).

(as well as residues from the leader peptides) were detected in 2D ^{13}C-HSQC spectra of Lchα and Lch*β*. These observations permit us to exclude the presence of impurities as a possible reason for the observed signal doubling. Thus, one can conclude that Lchα and Lch*β* in methanol solution experience structural fluctuations with characteristic times above hundred milliseconds between five and three conformational states, respectively. Most probably, the observed exchange processes involve cis−trans isomerization of partially double CO−CO and CO−NH bonds in the N-terminal OBu residues in both peptides and cis−trans isomerization of the Lys11-Pro12 peptide bond in Lchα. At the same time, involvement of more complex structural transitions (e.g., slow fluctuations in conformation of Lan and MeLan rings) cannot be ruled out. Interestingly, the observed conformational exchange processes do not strongly depend on the polarity and nature of the environment. For example, characteristic doubling of $^{1}H^{N}$ resonances of Dha5 and Dhb6 residues were detected in NMR spectra of Lchα in the solvent mixtures ranging from polar H_2O/CD_3OH (3:1) to strongly hydrophobic $CD_3OH/CDCl_3$ (2:3) (Figure S4, Supporting Information).

In spite of the presence of considerable signal doubling, the NMR spectra of Lchα and Lch*β* were relatively well dispersed and demonstrated narrow lines. This permitted us to implement further structural characterization of the major conformational state for both peptides. The qualitative analysis of $^{13}C^{\alpha}$ secondary chemical shifts ($\Delta\delta^{13}C^{\alpha}$) and NOE connectivity patterns (Figure 4E) revealed that Lchα in solution includes two structured domains (residues 2−10 and 22−32) connected with a flexible loop enclosed by a thioether bridge of Ala11-S-Ala21. The absence of medium- and long-range NOE contacts and vanishing $\Delta\delta^{13}C^{\alpha}$ values in this region of the peptide are probably due to the mobility of the Ala11-S-Ala21 loop in a nanosecond−picosecond time scale. In contrast to that, characteristic (i, i + 3) NOE connectivities and large positive $\Delta\delta^{13}C^{\alpha}$ values revealed the helical nature of the fragment of Lch*β* spanning residues 9−23 (Figure 4F). According to the NMR data, this helix is preceded by the more flexible N-terminal domain and followed by the structured C-terminal domain which contains two MeLan residues (Abu25-S-Ala28 and Abu29-S-Ala32). The trans-orientation of all X-Pro peptide bonds (two in each peptide) in the major conformational state was established on the basis of the sequential NOE cross-peaks (*19*).

The sets of 20 Lchα and Lch*β* structures were calculated in the program CYANA (*14*) using upper and lower NOE based distance constraints, as well as *J*-coupling based torsion angle constraints. The obtained structural ensembles for Lchα and Lch*β* together with representative conformers in ribbon representation are shown in Figure 6, and the structural statistics for

them are listed in Tables S6 and S7 (Supporting Information). The results of structure calculation were in agreement with the qualitative analysis of the NMR data (see above) and confirm the segregation of the peptides into differently structured domains. The structure of the mobile central loop in Lchα was weakly defined by the NMR data (Figure 6D), and more importantly, all three domains of Lchα have significantly different relative orientation in the calculated structural ensemble. This observation points to the presence of flexible hinges at AlaS11 and AlaS21 residues. Contrary to the situation observed for Lchα, the central domain of Lch*β* contains a well-structured prolonged α-helix (residues 9−22) flanked by two Lan (Ala7-S-Ala11 and Ala19-S-Ala23). The structure of this domain is more tightly defined by experimental data as compared to the N-terminal and C-terminal domains (Figure 6B), which points to the increased flexibility of the Lch*β* termini.

DISCUSSION

Comparison of Lichenicidin Gene Clusters in Different Strains of Bacillus licheniformis. Complete genome sequences of the *Bacillus licheniformis* ATCC14580 and DSM13 were determined earlier (ACCT14580, GenBank accession number GP000002 (*13*); DSM13, GenBank accession number AE017333 (*20*)). A putative gene cluster of a lantibiotic, named lichenicidin, has been annotated (*10*, *11*). In this work, two structural genes, *lchA1* and *lchA2*, encoding the lantibiotic precursors LchA1 and LchA2, and the *lchM1* gene, encoding a modifying bifunctional enzyme LchM1, were found in the lantibiotic cluster of the *Bacillus liheniformis* VK21 genome and sequenced. Comparison of nucleotide sequences of the corresponding clusters of *Bacillus licheniformis* VK21 and ATCC14580 demonstrated that these parts of the genomes are rather conservative in both strains. While the genes of lantibiotic precursors are completely identical, the *lchM1* gene contains 9 point mismatches (Table S1, Supporting Information). Four of them are synonymic and five result in amino acid substitutions. The character of these mismatches suggests that they take place due to a natural mutagenesis process rather than due to PCR errors. By analogy with other currently known two-component lantibiotics, LchM1 enzyme is likely responsible for the dehydration of Ser and Thr residues and subsequent cyclization to form thioether rings of Lan and MeLan residues.

Mechanism of the Lchα and Lchβ Maturation. Sequencing of the lichenicidin gene cluster of the *B. licheniformis* VK21 genome together with the determination of chemical structures of Lchα and Lch*β* allows us to propose mechanisms of the lantibiotic maturation (Figures 5A,B). For all known two-component lantibiotics, two different bifunctional enzymes are responsible for dehydration and subsequent cyclization of each prepeptide (*7*, *21*). In the lichenicidin VK21 two-component system, the intracellular LchM1 and LchM2 modifying enzymes likely catalyze dehydratation and cyclization of the corresponding prepeptides LchA1 and LchA2. These reactions result in the formation of four thioether rings and several Dha and Dhb residues in each peptide. The absence of additional post-translational conversion of Dha to D-Ala, previously observed in lacticin 3147 (*22*), correlates well with the absence of the LanJ enzyme gene in the *B. licheniformis* ATCC14580 genome (*13*). The second step of Lchα and Lch*β* maturation possibly involves secretion and N-terminal proteolysis by the multifunctional enzyme LchT (Figures 5A,B). Putative leader peptides with a double-glycine motif were identified in the lichenicidin VK21 precursors, LchA1 and LchA2. The leader peptides are most probably cleaved at the motif Gly-Gly, which is the lanT protease cleavage site in BhtA2, SmbA2, and LtnA2 (*23*). It is worthy of note that an additional 6-residue fragment (NDVNPE) following the Gly-Gly motif was found in the leader peptide of LchA2; thus, an additional proteolytic cleavage of six N-terminal residues is needed for the maturation of Lch*β*. The analysis of prepeptide sequences of different two-component lantibiotics revealed that additional proteolysis takes place in the case of plantaricin W and haloduracin maturation (*23*). A recent study of haloduracin two-component systems convincingly showed that an additional N-terminal proteolytic step must occur in Hal*β* (*9*). A similar processing step appears to be involved in the maturation of Lch*β*. Maturation of the lichenicidin VK21 peptides includes the formation of the N-terminal 2-oxobutyryl group. It is formed after spontaneous deamination of dehydrobutyrine, which is not stable in the N-terminal position. Conversion of the N-terminal Dhb to OBu has been previously studied in detail for lantibiotic Pep5 (*24*).

Chemical Structure: Comparison of Lchα and Lchβ with Other Two-Component Lantibiotics. Six two-component lantibiotics are presently known (see Introduction), and most of them were characterized just by the precursors gene sequencing. Only lacticin 3147, Ltnα and Ltn*β* from *Lactococcus lactis* DPC3147, and haloduracin, Halα and Hal*β* from *Bacillus halodurans* C-125 were studied at the level of chemical structure of the mature peptides with total characterization of post-translational modifications. Chemical structures of Ltnα and Ltn*β* were determined by extensive NMR analysis (*8*), and those of Halα and Hal*β* were deduced by mass-spectrometry and mutagenesis data combination (*9*). The presently described lichenicidin VK21 represents the third two-component lantibiotic with completely determined chemical structures of the mature peptides, Lchα and Lch*β*. Comparison of amino acid sequences of the lichenicidin VK21 precursors and mature peptides with other two-component lantibiotics and the single-component lantibiotic mersacidin (Mrs) shows observable homology in the propeptide region and, at the same time, reveals distinct features of Lchα and Lch*β* (Figures 1B,C and 5C). First of all, the N-terminal fragment of Lchα contains a 5-residue MeLan ring A that was not observed previously in α-components of lantibiotics. Second, the N-terminal fragment of Lch*β* contains a 5-residue Lan ring A which closely resembles the N-terminal MeLan ring of Hal*β*, but in Lch*β*, this ring is preceded by a 6-residue linear fragment that has essential sequence homology with the N-terminal fragment of Ltn*β*. Interestingly, Ltn*β* does not contain thioether ring A at all. Finally, both Lchα and Lch*β* are N-terminally blocked by the 2-oxobutyryl group similar to the Ltn*β* component of lacticin 3147. In contrast to the observed variability in the N-terminal thioether rings, structures of the B, C, and D rings in α- and *β*-components of lichenicidin VK21, lacticin 3147, and haloduracin are rather similar to each other. Lchα is most homologous to Ltnα, Halα, and Mrs in the region of the C and D rings including functionally important Glu involved in lipid II binding (*25*) (Figure 5C). Besides, there is a conservative palindromic group of four amino acid residues (Gly, Asn, Asn, and Gly) inside the B rings of Lchα and Ltnα. Interestingly, the ring A in Lchα shares some structural similarity with the N-terminal thioether ring in a single-component lantibiotic nisin A (Figure 5C). It is worth noting that this ring in nisin A (Nis) forms the site for lipid II binding (*26*). The determined primary structures of the mature peptides, Lchα and Lch*β*,

significantly differ from those of Bliα and Bliβ from *Bacillus lichenifromis* ATCC 14580 predicted using the lacticin 3147 components Ltnα and Ltnβ as templates (*10*).

Antimicrobial Effects and Synergy. Individual Lchα and Lchβ inhibit Gram-positive bacteria at micromolar concentrations with target-dependent effectiveness (Table 1). *Micrococcus luteus*, strain B1314, and *Bacillus megaterium*, strain VKM41, were the most sensitive test microorganisms. Neither individual peptides nor their mixtures inhibit Gram-negative bacteria growth. The liquid media growth assay revealed the specific activity of the two-component lantibiotic lichenicidin VK21, corresponding to a 20- to 50-fold higher efficacy as compared to that of each individual peptide, Lchα or Lchβ (Table 1). The mixture of Lchα and Lchβ at a 1:1 ratio displayed antimicrobial activity within the nanomolar concentration range. Thus, lichenicidin VK21 was found to be a novel two-component lantibiotic exhibiting much higher biological activity in synergy.

We determined an optimum ratio of the individual Lchα and Lchβ in the double-component system as the ratio of Lchα and Lchβ that yields maximum biological activity. Effects of the Lchα and Lchβ mixtures on *Bacillus megaterium* VKM41 growth at varying concentrations and ratios of the peptides were established. As indicated in Figure 3F, Lchα and Lchβ display maximum activity at a 1:1 ratio. The optimal synergistic effect of α- and β-peptides of two-component lantibiotics at a 1:1 ratio was demonstrated earlier for staphylococcin C55 (*2*), plantaricin W (*4*), lacticin 3147 (*27*), and haloduracin (*28*).

Functional and Structural Data Provide Insight into the Mode of Lichenicidin VK21 Action. A modern concept in the molecular mechanism of antibacterial action of a two-component lantibiotic was proposed on the basis of structural NMR investigation of lacticin 3147 peptides (*8*). It was further supported by extensive mutagenesis and structure−function studies of lacticin 3147 (*29*) and haloduracin (*9*, *28*). According to this concept, membrane-mediated antibacterial action of two-component lantibiotics includes several steps. At the first stage, the α-component selectively binds lipid II, a central component in bacterial wall synthesis. The second step is selective binding of a more elongated and helical β-component to the complex α-component/lipid II in a 1:1 stoichiometry and formation of ion-conducting pores in the membrane of the target cell. In turn, the pore formation leads to cell death.

By now, two different lipid II binding motifs were identified in lantibiotics (*30*). The first type, found in nisin and Nis-like peptides (gallidermin, epidermin, mutacin 1140, and subtillin), interacts with lipid II as a docking molecule whereby preventing its further incorporation in cell wall biosynthesis. It was shown by NMR spectroscopy that lipid II interacts with the A and B rings of Nis forming a cage with five intermolecular hydrogen bonds between Nis backbone amides and oxygen atoms of pyrophosphate (Figure 6F) (*26*). Comparison of the determined Lchα spatial structure with the structure of Nis in complex with lipid II reveals close similarity in the conformation of a five-residue thioether ring A with backbone rmsd of about 0.76 Å for the Abu3-S-Ala7 region of Lchα and corresponding region of Nis. The observed similarity is significant: as a comparison, the 5-residue thioether rings A and B of Lchβ display a much larger rmsd value (of about 1.2 Å) with the ring A of Nis. Superimposition of the Lchα spatial structure with that of Nis/lipid II complex revealed at least three hydrogen bonds that could be formed between backbone amides of Lchα and oxygen atoms of pyrophosphate (Figure 6F). At the same time, several sterical clashes were observed between the atoms of Lchα and the pyrophosphate moiety of lipid II. Nevertheless, keeping in mind the large flexibility of the N-terminal fragment of Lchα, which can adopt up to five different conformations in methanol solution (see above), we assume that some adaptation in conformation of thioether ring A can lead to the formation of the energetically favorable complex Lchα/lipid II.

The second lipid II binding motif was found in the C-terminal domains of mersacidin and Mrs-related lantibiotics (plantaricin C, lacticin 481, and in α-component of lacticin 3147 and haloduracin (Figure 5C)). Although the ability of Mrs to specifically bind lipid II and inhibit the transglycosylation step of peptidoglycan biosynthesis is well documented (*31*, *32*), molecular details of this interaction are presently unknown. Comparison of the Lchα spatial structure in solution with the crystal structure of Mrs (*33*) reveals close similarity of the proposed lipid II binding domains. Indeed, both peptides demonstrate very similar conformation of the thioether ring C with backbone rmsd of about 0.41 Å for the Abu22-S-Ala27 region of Lchα and the corresponding region of Mrs (Figures 6C,E). The spatial position of the Glu26 charged side-chain is also well preserved. It is worth noting that this residue is fully conserved in Mrs-like peptides, including α-components of two-peptide lantibiotics. The side chain of Glu17 of Mrs was proposed to participate in lipid II binding, and its replacement by Ala makes Mrs inactive (*25*). There are also some similarities in the dynamic behavior of Lchα and Mrs. The current structural investigation of Lchα revealed the presence of a flexible hinge between AlaS21 and AbuS22 residues. This hinge controls a relative spatial arrangement of the thioether rings B and C in solution. Interestingly, a similar hinge region in Mrs was previously described on the basis of NMR data (*25*). Significant changes in the hinge conformation and, as a consequence, relative orientation of the B and C rings were observed in Mrs upon lipid II binding. Taking together all the structural evidence, we can presume that Lchα shares with other Mrs-like peptides the same lipid II binding mechanism.

The presently obtained functional and structural data prompts us to conclude that the mechanism of antibacterial action of lichenicidin VK21 is very similar to mechanisms previously described for other two-component lantibiotics. Most probably, Lchα binds lipid II molecules using either one or both of its putative lipid II binding sites. Subsequent involvement of Lchβ in this complex in 1:1 stoichiometry is likely to moderate its insertion into a targeted membrane that results in pore formation. This model is supported by a wealth of experimental evidence. First of all, the Lchα/Lchβ system displays antibacterial activity in the nanomolar concentration range, thus implying the presence of a specific molecular target in the membrane of the susceptible cell. The close structural similarity between N- and C-terminal domains of Lchα and lipid II binding motifs of other lantibiotics points to lipid II as a most likely molecular target for Lchα binding. Second, the central domain of Lchβ represents a hydrophobic helix with length of ~23 Å (Figure 6A) that is sufficient to span hydrocarbon regions of a lipid bilayer. Finally, the proposed model is strongly supported by the data on the synergistic effect of Lchα and Lchβ, which is maximal at a 1:1 ratio (Figure 3F). The obtained structural data also permit us to propose the mechanisms of the relatively weak antibacterial activity of individual Lchα and Lchβ peptides. Most probably, the interaction of Lchα with lipid II could inhibit peptidoglycan biosynthesis. Similar to Ltnβ and Halβ, the cationic Lchβ may bind to anionic lipids of the bacterial cell membrane and cause the

transient pore formation via a nisin-like mechanism developing in the absence of lipid II (*34*).

ACKNOWLEDGMENT

We thank Evgeniy N. Nikolaev and co-workers (Laboratory for Mass-Spectrometry of Biomacromolecules, Emanuel Institute of Biochemical Physics, Russian Academy of Sciences, Moscow, Russia) for performing MS experiments, and Elena I. Shramova (Shemyakin & Ovchinnikov Institute of Bioorganic Chemistry, Russian Academy of Sciences, Moscow, Russia) for assistance in genes sequence analysis.

SUPPORTING INFORMATION AVAILABLE

NMR spectra, ^{1}H,^{13}C chemical shifts, *J* coupling constants, statistics of spatial structure calculation, MS and MS/MS data for Lchα and Lch*β* peptides, and nucleotide mismatches in the *lchM1* genes of different *Bacillus licheniformis* strains. This material is available free of charge via the Internet at http://pubs.acs.org.

REFERENCES

1. Asaduzzaman, S. M., and Sonomoto, K. (2009) Lantibiotics: diverse activities and unique modes of action. *J. Biosci. Bioeng. 107*, 475–487.
2. Navaratna, M. A., Sahl, H. G., and Tagg, J. R. (1998) Two-component anti-Staphylococcus aureus lantibiotic activity produced by Staphylococcus aureus C55. *Appl. Environ. Microbiol. 64*, 4803–4808.
3. Ryan, M. P., Jack, R. W., Josten, M., Sahl, H. G., Jung, G., Ross, R. P., and Hill, C. (1999) Extensive post-translational modification, including serine to D-alanine conversion, in the two-component lantibiotic, lacticin 3147. *J. Biol. Chem. 274*, 37544–37550.
4. Holo, H., Jeknic, Z., Daeschel, M., Stevanovic, S., and Nes, I. V. (2001) Plantaricin W from *Lactobacillus plantarum* belongs to a new family of two-peptide lantibiotics. *Microbiology 147*, 643–651.
5. Yonezawa, H., and Kuramitsu, H. K. (2005) Genetic analysis of a unique bacteriocin, Smb, produced by *Streptococcus* mutants GS5. *Antimicrob. Agents Chemother. 49*, 541–548.
6. Hyink, O., Balakrishnan, M., and Tagg, J. R. (2005) *Streptococcus rattus* strain BHT produces both a class I two-component lantibiotic and a class II bacteriocin. *FEMS Microbiol. Lett. 15*, 235–241.
7. McClerren, A. L., Cooper, L. E., Quan, C., Thomas, P. M., Kelleher, N. L., and van der Donk, W. A. (2006) Discovery and *in vitro* biosynthesis of haloduracin, a new two-component lantibiotic. *Proc. Natl. Acad. Sci. U.S.A. 103*, 17243–17248.
8. Martin, N. I., Sprules, T., Carpenter, M. R., Cotter, P. D., Hill, C., Ross, R. P., and Vederas, J. C. (2004) Structural characterization of lacticin 3147, a two-peptide lantibiotic with synergistic activity. *Biochemistry 43*, 3049–3056.
9. Cooper, L. E., McClerren, A. L., Chary, A., and van der Donk, W. A. (2008) Structure-activity relationship studies of the two-component lantibiotic haloduracin. *Chem. Biol. 15*, 1035–1045.
10. Begley, M., Cotter, P. D., Hill, C., and Ross, R. P. (2009) Identification of a novel two-peptide lantibiotic, lichenicidin, following rational genome mining for LanM proteins. *Appl. Environ. Microbiol. 75*, 5451–5460.
11. Dischinger, J., Josten, M., Szekat, C., Sahl, H.-G., and Bierbaum, G. (2009) Production of the novel two-peptide lantibiotic lichenicidin by *Bacillus licheniformis* DSM 13. *PLoS One 26*, e6788.
12. Sambrook, J., Russel, D. W. (2001) Molecular Cloning: A Laboratory Manual, Cold Spring Harbor Laboratory Press, New York.
13. Rey, M. W., Ramaiya, P., Nelson, B. A., Brody-Karpin, S. D., Zaretsky, E. J., Tang, M., Lopez de Leon, A., Xiang, H., Gusti, V., and Clausen, I. G.; et al. (2004) Complete genome sequence of the industrial bacterium *Bacillus licheniformis* and comparisons with closely related *Bacillus* species. *Genome Biol. 5*, R77.
14. Herrmann, T., Guntert, P., and Wuthrich, K. (2002) Protein NMR structure determination with automated NOE assignment using the new software CANDID and the torsion angle dynamics algorithm DYANA. *J. Mol. Biol. 319*, 209–227.
15. Ovchinnikova, T. V., Aleshina, G. M., Balandin, S. V., Krasnosdembskaya, A. D., Markelov, M. L., Frolova, E. I., Leonova, Y. F., Tagaev, A. A., Krasnodembsky, E. G., and Kokryakov, V. N. (2004) Purification and primary structure of two isoforms of arenicin, a novel antimicrobial peptide from marine polychaeta *Arenicola marina*. *FEBS Lett. 577*, 209–214.
16. Ovchinnikova, T. V., Shenkarev, Z. O., Nadezhdin, K. D., Balandin, S. V., Zhmak, M. N., Kudelina, I. A., Finkina, E. I., Kokryakov, V. N., and Arseniev, A. S. (2007) Recombinant expression, synthesis, purification, and solution structure of arenicin. *Biochem. Biophys. Res. Commun. 360*, 156–162.
17. Dewan, P. C., Anantharaman, A., Chauhan, V. S., and Sahal, D. (2009) Antimicrobial action of prototypic amphipathic cationic decapeptides and their branched dimers. *Biochemistry 48*, 5642–5657.
18. Cavanagh, J., Fairbrother, W. J., Palmer, A. G., III, Skelton, N. J., and Rance, M. (2006) Protein NMR Spectroscopy: Principles and Practice, 2nd ed., Academic Press, New York.
19. Wuthrich, K. (1986) NMR of Proteins and Nucleic Acids, John Wiley and Sons, New York.
20. Veith, B., Herzberg, C., Steckel, S., Feeshe, J., Maurer, K. H., Ehrenreich, P., Bäumer, S., Henne, A., Liesegang, H., Merkl, R., Ehrenreich, A., and Gottschalk, G. (2004) The complete genome sequebce of *Bacillus licheniformis* DSM13, an organism with great industrial potential. *J. Mol. Microbiol. Biotechnol. 7*, 204–211.
21. McAuliffe, O., Hill, C., and Ross, R. P. (2000) Each peptide of the two-component lantibiotic lacticin 3147 requires a separate modification enzyme for activity. *Microbiology 146*, 2147–2154.
22. Cotter, P. D., O'Connor, P. M., Draper, L. A., Lawton, E. M., Deegan, L. H., Hill, C., and Ross, R. P. (2005) Posttranslational conversion of L-serines to D-alanines is vital for optimal production and activity of the lantibiotic lacticin 3147. *Proc. Natl. Acad. Sci. U.S.A. 102*, 18584–18589.
23. Willey, J. M., and van der Donk, W. A. (2007) Lantibiotics: peptides of diverse structure and function. *Annu. Rev. Microbiol. 61*, 477–501.
24. Kaletta, C., Entian, K.-D., Kellner, R., Jung, G., Reis, M., and Sahl, H.-G. (1989) Pep5, a new lantibiotic: structural gene isolation and prepeptide sequence. *Arch. Microbiol. 152*, 16–19.
25. Hsu, S. T., Breukink, E., Bierbaum, G., Sahl, H.-G., de Kruijff, B., Kaptein, R., van Nuland, N. A., and Bonvin, A. M. (2003) NMR study of mersacidin and lipid II interaction in dodecylphosphocholine micelles. *J. Biol. Chem. 278*, 13110–13117.
26. Hsu, S. T., Breukink, E., Tischenko, E., Lutters, M. A., de Kruijff, B., Kaptein, R., Bonvin, A. M., and van Nuland, N. A. (2004) The nisin-lipid II complex reveals a pyrophosphate cage that provides a blueprint for novel antibiotics. *Nat. Struct. Mol. Biol. 11*, 963–967.
27. Morgan, S. M., O'Connor, P. M., Cotter, P. D., Ross, R. P., and Hill, C. (2005) Sequential actions of the two component peptides of the lantibiotic lacticin 3147 explain its antimicrobial activity at nanomolar concentrations. *Antimicrob. Agents Chemother. 49*, 2606–2611.
28. Oman, T. J., and van der Donk, W. A. (2009) Insights into the mode of action of the two-peptide lantibiotic haloduracin. *ACS Chem. Biol. 4*, 865–874.
29. Field, D., Collins, B., Cotter, P. D., Hill, C., and Ross, R. P. (2007) A system for the random mutagenesis of the two-peptide lantibiotic lacticin 3147: analysis of mutants producing reduced antibacterial activities. *J. Mol. Microbiol. Biotechnol. 13*, 226–234.
30. Bierbaum, G., and Sahl, H. G. (2009) Lantibiotics: mode of action, biosynthesis and bioengineering. *Curr. Pharm. Biotechnol. 10*, 2–18.
31. Brötz, H., Bierbaum, G., Reynolds, P. E., and Sahl, H. G. (1997) The lantibiotic mersacidin inhibits peptidoglycan biosynthesis at the level of transglycosylation. *Eur. J. Biochem. 246*, 193–199.
32. Brötz, H., Bierbaum, G., Leopold, K., Reynolds, P. E., and Sahl, H. G. (1998) The lantibiotic mersacidin inhibits peptidoglycan synthesis by targeting lipid II. *Antimicrob. Agents Chemother. 42*, 154–160.
33. Schneider, T. R., Kärcher, J., Pohl, E., Lubini, P., and Sheldrick, G. M. (2000) Ab initio structure determination of the lantibiotic mersacidin. *Acta Crystallogr., Sect. D 56*, 705–713.
34. Breukink, E., and de Kruijff, B. (2006) Lipid II as a target for antibiotics. *Nat. Rev. Drug Discovery 5*, 321–332.
35. Koradi, R., Billeter, M., and Wuthrich, K. (1996) MOLMOL: a program for display and analysis of macromolecular structures. *J. Mol. Graphics 14*, 51–55.